

blood

2010 116: 2183-2191
Prepublished online June 10, 2010;
doi:10.1182/blood-2010-03-276170

A revised model for the secretion of tPA and cytokines from cultured endothelial cells

Laura Knipe, Athinoula Meli, Lindsay Hewlett, Ruben Bierings, John Dempster, Paul Skehel, Matthew J. Hannah and Tom Carter

Updated information and services can be found at:
<http://bloodjournal.hematologylibrary.org/content/116/12/2183.full.html>

Articles on similar topics can be found in the following Blood collections
[Vascular Biology](#) (249 articles)

Information about reproducing this article in parts or in its entirety may be found online at:
http://bloodjournal.hematologylibrary.org/site/misc/rights.xhtml#repub_requests

Information about ordering reprints may be found online at:
<http://bloodjournal.hematologylibrary.org/site/misc/rights.xhtml#reprints>

Information about subscriptions and ASH membership may be found online at:
<http://bloodjournal.hematologylibrary.org/site/subscriptions/index.xhtml>



A revised model for the secretion of tPA and cytokines from cultured endothelial cells

Laura Knipe,¹ Athinoula Meli,¹ Lindsay Hewlett,¹ Ruben Bierings,¹ John Dempster,² Paul Skehel,³ Matthew J. Hannah,¹ and Tom Carter¹

¹Medical Research Council, National Institute for Medical Research, London; ²Department of Physiology and Pharmacology, University of Strathclyde, Glasgow; and ³Centre for Integrative Physiology, University of Edinburgh, Edinburgh, United Kingdom

Endothelial cells are reported to contain several distinct populations of regulated secretory organelles, including Weibel-Palade bodies (WPBs), the tissue plasminogen activator (tPA) organelle, and the type-2 chemokine-containing organelle. We show that the tPA and type-2 organelles in human endothelial cells represent a single compartment primarily responsible for unstimulated secretion of tPA or, in cells exposed to interleukin-1 β (IL-1 β), the cytokines IL-8, IL-6, monocyte chemoattractant protein-1 (MCP-1), and

growth-regulated oncogene- α (GRO- α). This compartment was distinct from WPBs in that it lacked detectable von Willebrand factor, P-selectin, Rab27a, or CD63 immunoreactivity, displayed no time-dependent decrease in intragranule pH, underwent detectable unstimulated exocytosis, and was very poorly responsive to Ca²⁺-elevating secretagogues. WPBs could also contain tPA, and in IL-1 β -treated cells, IL-8, IL-6, MCP-1, and GRO- α , and were the primary source for histamine or ionomycin-stimulated secre-

tion of these molecules. However, analysis of the storage efficiency of cytokines and tPA revealed that all were very poorly stored compared with von Willebrand factor. The nonmammalian, nonsecretory protein EGFP, when expressed in the secretory pathway, also entered WPBs and had a storage efficiency similar to tPA and the cytokines tested. Based on these data, we proposed a revised model for storage and secretion of cytokines and tPA. (*Blood*. 2010;116(12):2183-2191)

Introduction

Several studies suggest that endothelial cells (ECs) possess several distinct populations of regulated secretory organelles (RSOs) in which different subsets of bioactive peptides and proteins are stored, trafficked, and rapidly secreted in response to physiologic stimuli. These include (1) Weibel-Palade bodies (WPBs) whose major cargo protein is von Willebrand factor (VWF)¹; (2) a small punctate organelle, morphologically distinct from WPBs, lacking endogenous VWF immunoreactivity but containing the anticoagulant protein tissue plasminogen activator (tPA; the tPA organelle)²⁻⁴; and (3) a small punctate organelle, reported to specifically contain the small chemotactic cytokines growth-regulated oncogene- α (GRO- α) and monocyte chemoattractant protein 1 (MCP-1) and termed the type-2 granule.⁵ The presence of distinct populations of RSOs within the same cell is not uncommon⁶⁻⁸ and may allow the stimulated release of diverse bioactive molecules to be differentially controlled. If distinct populations of RSOs do exist in ECs, then a careful examination of their properties would provide insights into how trafficking and secretion of specific groups of bioactive molecules are regulated.

WPBs are the best characterized RSO of ECs. After their formation at the trans-Golgi network (TGN), WPBs accumulate in the cytoplasm and can remain within the cell for long periods of time (1-2 days).^{9,10} By these criteria, we define WPBs as true storage organelles. Under resting conditions, WPBs undergo a very slow process of basal exocytosis,¹⁰ undetectable in optical recordings from individual live cells.¹¹ However, their rate of exocytosis is rapidly increased in response to external stimuli that elevate

intracellular free calcium ion concentrations ($[Ca^{2+}]_i$).¹¹ A punctate tPA-containing organelle has been described as the tPA-storage organelle in endothelium,² from which stimulated tPA secretion is proposed to arise.^{2,3,12} However, tPA may also reside within WPBs,^{3,12,13} and uncertainty still remains as to which of these 2 compartments is primarily responsible for stimulated tPA secretion. The properties of the tPA-storage organelle remain poorly defined. Is it, like the WPB, a true long-term storage organelle, and can it undergo robust stimulated exocytosis? Optical studies show that the tPA organelle undergoes significant unstimulated exocytosis,¹⁴ suggesting that they are not retained within the cell as efficiently as WPBs under resting conditions.¹¹ Direct optical analysis of the kinetics and extent of stimulated exocytosis of the tPA organelle are still lacking. The type-2 chemokine-containing organelle is morphologically similar to the tPA organelle, but the lack of colocalization of overexpressed tPA with punctate GRO- α -containing organelles led to the conclusion that they comprised a distinct population of RSOs.⁵

We have reexamined the composition and properties of the tPA organelle, the type-2 chemokine-containing organelle, and WPBs in human umbilical vein endothelial cells (HUVECs). From these data, we propose a revised model for secretion of tPA and cytokines from ECs. We question whether cytokines, detectable in WPBs under conditions where their expression levels are up-regulated, are sorted to this cellular compartment. Instead, we suggest that such molecules are efficiently excluded from WPBs and that their presence in WPBs arises from an exclusion mechanism that is almost, but not quite, 100% efficient.

Submitted March 22, 2010; accepted June 3, 2010. Prepublished online as *Blood* First Edition paper, June 10, 2010; DOI 10.1182/blood-2010-03-276170.

The publication costs of this article were defrayed in part by page charge payment. Therefore, and solely to indicate this fact, this article is hereby marked "advertisement" in accordance with 18 USC section 1734.

The online version of this article contains a data supplement.

© 2010 by The American Society of Hematology

Methods

Tissue culture and transfection

Primary HUVECs were purchased, grown, Nucleofected (Lonza Cologne AG), plated, and maintained for live-cell imaging or immunofluorescence as previously described.^{15,16} Cells were used between 6 and 48 hours after Nucleofection depending on the experiment.

Antibodies, reagents, immunocytochemistry, and confocal microscopy

Reagents were purchased from Sigma-Aldrich unless stated otherwise. tPA-EGFP, proregion-EGFP, and proregion-mRFP were made as previously described.¹⁵⁻¹⁷ Human Rab6, Rab8, Rab10, Rab11, and Rab27a cDNAs (cDNA Resource Center; www.cdna.org) were ligated as *HindIII*/*Apal* fragments into Myc-C3 to generate N-terminally Myc-tagged versions. Myc-C3 was derived from EGFP-C3 (Clontech) by removing the EGFP cDNA using *AgeI*/*BsrGI* and inserting the MYC epitope coding sequence using a double-stranded linker made by annealing the oligos 5'-ccggatgcatcaatgcagaagctgatctcagaggaggacct-3' (forward) and 5'-gtacagctcctctctcagatcagcttctcattgatgcata-3' (reverse). Human Rab27a cDNA was cloned into mRFP-C3 as a *HindIII*/*Apal* fragment to make mRFP-hRab27a. mRFP-C3 was constructed from EGFP-C3 by exchanging the fluorophore encoding region with a *AgeI*/*BsrGI* fragment of PCR amplified mRFP1 described previously.¹⁸ LumEGFP was cut from a vector provided by Dr David Stevens (University of Bristol, Bristol, United Kingdom¹⁹) and recloned into *NheI*/*BsrGI* digested pEGFP-N1 (Clontech). Human interleukin-8 (IL-8; image ID 3882471) and GRO- α (image ID 3856841) image clones were from Geneservice. Rabbit anti-human VWF was from Dako. A sheep antihuman VWF antibody, a mouse antihuman VWF antibody (MCA127), a sheep anti-tPA antibody, a sheep anti-GFP antibody, and a mouse anti-P-selectin antibody (AK6) were from AbD Serotec. The antibodies H4A3 (to LAMP-1) and H5C6 (to CD63), developed by J.T August and J.E.K. Hildreth, were from the Developmental Studies Hybridoma Bank, developed under National Institute of Child Health and Human Development and maintained by the University of Iowa (Iowa City, IA). An antibody to the transferrin receptor (H64.8) was from Zymed Laboratories. A rabbit anti-GFP antibody was from Invitrogen. Recombinant human IL-1 β (rhIL-1 β), rhIL-4, goat antibodies to human IL-6, IL-8, MCP-1, and eotaxin-3, and a mouse antibody to human GRO- α (clone 20326) were from R&D Systems. rhIL-6, rhIL-8, and a rabbit antibody to human GRO- α were from PeproTech. Rab27a antibody was from BD Transduction Laboratories (catalog no. 610595/6). Fluorophores or horseradish peroxidase (HRP)-coupled secondary antibodies were from Jackson ImmunoResearch Laboratories. Donkey anti-goat IgG coupled to IR800 was from LI-COR. Single optical section confocal images of fixed cells mounted in mowiol (Harlow Chemical Company Ltd) were acquired using a Leica TCS-SP2 confocal microscope equipped with a PLAPO 100 \times /1.4 numeric aperture oil objective and Leica Version 2.61 software as previously described.¹⁸ Images at different excitation wavelengths were acquired sequentially with 14 to 25 frame averaging using nonsaturating excitation and electronic zoom 1-25 \times . Images were exported to and processed in Adobe Photoshop CS4 Version 11.0.

Stimulation protocols and ELISAs

Endogenous cytokines were up-regulated by incubating with rhIL-1 β (24 hours or 48 hours, 1 ng/mL) or rhIL-4 (24 hours, 20 ng/mL) in full growth medium (HGM). For experiments with brefeldin-A (BFA), cells were transferred into serum and bicarbonate-free M199 (Invitrogen), containing 20mM N-2-hydroxyethylpiperazine-N'-2-ethanesulfonic acid (pH 7.4) and 5 μ M BFA or vehicle (0.05% EtOH) and incubated for 60 minutes before fresh media (with BFA or vehicle) was exchanged. Ten minutes later, fresh media containing 100 μ M histamine or vehicle was added, and this was collected 10 minutes later for assay. For cycloheximide (CHX) experiments, cells were transferred into fresh HGM containing rhIL-1 β and 5 μ M CHX or vehicle control and cultured for a further 24 hours. Cells were then transferred into serum and bicarbonate-free M199

and treated as described for BFA-treated cells (see earlier in this paragraph), except 5 μ M CHX replaced BFA, and cells were stimulated with 100 μ M histamine, 2 μ M ionomycin, or vehicle. All medium and lysate samples were prepared and stored as previously described.¹⁸

IL-8, IL-6, MCP-1, or GRO- α from media or lysate samples was assayed in triplicate using commercial enzyme-linked immunosorbent assay (ELISA) kits (human IL-8 and GRO- α kits from Antigenix America, PeIKine compact human IL-6 kit from Sanquin, and human MCP-1 and GRO- α kits from PeproTech). ELISAs were performed according to the manufacturer's instructions, with the exception that washes and blocking were carried out using a Tween-ELISA buffer (phosphate-buffered saline containing 0.1% Tween-20, 0.2% gelatin, and 1mM ethylenediaminetetraacetic acid). Streptavidin-HRP was either included in the ELISA kits or was from Jackson ImmunoResearch. HRP activity was detected colorimetrically using a 0.15% (wt/vol) solution of o-phenyldiamine dihydrochloride in a citrate/phosphate buffer containing 1% Triton X-100 and 0.012% (weight/volume) H₂O₂ added just before use. Absorbance was recorded using a VERSAmax microplate reader (MDS Analytical Technologies). Standard curves were made in serum-free N-2-hydroxyethylpiperazine-N'-2-ethanesulfonic acid-buffered M199 or in lysis buffer. EGFP was assayed using a sandwich ELISA. Plates were coated with a sheep anti-GFP antibody. Bound GFP was detected with a rabbit anti-GFP followed by a donkey anti-rabbit HRP-conjugated secondary. Standard curves were made from dilutions of recombinant bacterially produced GFP. tPA from media samples were assayed by sandwich ELISA. Plates were coated with a sheep anti-tPA coating antibody (Serotec). Bound tPA was detected with a sheep anti-tPA-HRP conjugate (Quadrantech). Standard curves were constructed in serum and bicarbonate-free M199 from a 1:10 dilution of HGM taken from HUVECs incubated for 24 hours with 3mM Na-butyrate.

Storage efficiency for IL-8, IL-6, MCP-1, GRO- α , VWF, tPA, and lumEGFP

A storage efficiency for IL-8, IL-6, MCP-1, GRO- α , and lumEGFP was estimated as follows. Cells were used after 24 hours of treatment with IL-1 β (1 ng/mL), at which time up-regulation of cytokine expression had reached a steady state. Under these conditions, cells were synthesizing cytokines at the same rate at which they are secreted (ie, there was a constant flux of material through all compartments),²⁰ with no additional accumulation of material in cell lysates or differences in secretion between 24 and 48 hours (supplemental Figure 1A, available on the *Blood* Web site; see the Supplemental Materials link at the top of the online article). At this point, cells were either placed in fresh media containing 5 μ M CHX (and IL-1 β) and cultured for a further 24 hours or treated for 1 hour with BFA (5 μ M), at which time cell lysates were harvested. BFA rapidly (within 5 minutes) disrupts endoplasmic reticulum (ER) to Golgi transport, preventing exit of newly synthesized material from the ER without affecting post-Golgi vesicle secretion (see Figure 5) and protein biosynthesis. Therefore, the amount of material accumulated in lysates during 1 hour of BFA treatment reflects the amount of material synthesized during that time period ("a" in supplemental Figure 1B; assuming no degradation), and the amount of material potentially synthesized in 24 hours can be estimated by multiplying this value ("a") by 24. Meanwhile, the amount of that material remaining within cells after 24 hours of exposure to CHX was defined as the stored material ("b" in supplemental Figure 1B). This use of BFA to estimate total synthetic capacity was used in preference to measuring accumulated material in cell lysates and media over a 24-hour period because of uncertainties over stability of secreted proteins in the media over such long time periods.¹⁰ Storage efficiency was estimated by taking the ratio of the stored material ("b") and the amount of material potentially synthesized in 24 hours ("a"). A storage efficiency for VWF, tPA, and lumEGFP was determined by pulse-chase and immunoprecipitation methods. For VWF and tPA, cells were metabolically labeled for 30 minutes (50 μ Ci/mL Expre³⁵S³⁵S protein labeling mix, PerkinElmer Life and Analytical Sciences), followed by incubation for 24 hours before harvesting media and lysates for immunoprecipitation of tPA and VWF. Immunoprecipitations on media and lysates were performed sequentially using a sheep anti-tPA antibody bound to protein G-Sepharose (Generon) followed by a

rabbit anti-VWF antibody (Dako) bound to protein A-Sepharose. Immunoprecipitates were eluted and run on a 10% gel (for tPA) or 6% gel (for VWF). Gels were stained, dried, and exposed to storage phosphor plates as described previously.¹⁰ For LumEGFP, cells were Nucleofected with LumEGFP 24 hours before ³⁵S labeling, followed by a further incubation of 24 hours before harvesting. EGFP immunoprecipitations used a rabbit anti-GFP antibody coupled to protein A-Sepharose, and the eluted immunoprecipitates were run on a 12% gel. Bands corresponding to VWF, tPA, or EGFP were quantified using ImageJ Version 1.41o software (<http://rsb.info.nih.gov/ij/>), and storage efficiency was calculated from material in cell lysates (after 24 hours) as a proportion of total material (lysate plus media).

Fluorescence imaging of tPA-granules in living HUVECs

Experiments to quantify the effect of BFA treatment on numbers of tPA-EGFP puncta or WPBs (labeled with proregion-EGFP) were carried out at 37°C using a DeltaVision Imaging system (Applied Precision) as previously described.^{15,16} Z-series image stacks composing 7 or 8 optical sections at 0.3-µm intervals were obtained approximately 3 minutes after addition of BFA or vehicle and subsequently every 3 to 5 minutes over the following approximately 60 to 90 minutes. The numbers of fluorescent tPA organelles or WPBs in the cell were determined as described in "Data analysis and measurements." Epifluorescence or total internal reflection fluorescence imaging of [Ca²⁺]_i and tPA organelle (tPA-EGFP) or WPB (proregion-EGFP) exocytosis was carried out in Fura-2-loaded cells as previously described¹¹ but using an Olympus UPLSAPO × 100 1.40NA objective. Cells coexpressing tPA-EGFP and either mRFP-hRab27a or proregion-mRFP (24 hours after Nucleofection) were sequentially illuminated at 355 plus or minus 7 nm, 380 plus or minus 7 nm (Fura-2), 470 plus or minus 20 nm (EGFP), and 555 plus or minus 20 nm (mRFP) using a monochromator (Cairn Research). A custom dichroic mirror (Chroma, 51019 + 400DCLP) and EGFP/DsRed dual-band emission filter were used. The custom-built objective-based total internal reflection fluorescence system^{21,22} was incorporated into the epifluorescence microscope with 488 nm (Point Source) and 561 nm laser light sources (GLC-050-561). Illumination was synchronized with image capture using Winfluor software (<http://spider.science.strath.ac.uk>). Images were acquired at 30 or 40 (reduced pixel area) frames/sec.

pH in the tPA organelle

The resting pH in tPA-EGFP-containing punctate organelles was determined from epifluorescence measurements of the steady-state fluorescence of EGFP and the maximum fluorescence of the organelle EGFP, obtained after acute application of the weak base ammonium chloride (NH₄Cl; 5-10mM), using parameters describing the relationship between EGFP fluorescence and pH determined previously (pK_a of 5.84 and n_H of 0.74¹¹). Resting pH within tPA-EGFP punctate granules was also determined from organelles undergoing exocytosis into extracellular media at pH 7.4 as previously described.¹¹

Data analysis and measurements

Image analysis was carried out in Winfluor (<http://spider.science.strath.ac.uk>) or ImageJ. The number of tPA-EGFP puncta or WPBs in cells during BFA treatment were counted manually using the ImageJ pointpicker plugin (<http://rsb.info.nih.gov/ij/plugins/index.html>). Optical sections at each point in time-lapse sequences were projected within pointpicker, allowing granules in different optical planes to be identified and marked. Numbers of granules at each time point were counted twice and the average taken. Extent of histamine or ionomycin-evoked degranulation was estimated as previously described.¹¹ Dataset plotting, fitting, and analysis were performed in Microcal Origin 7.5 (OriginLab Corporation). Results are expressed as mean plus or minus SD unless indicated otherwise. Statistical differences (at 95% confidence limit) between population means were determined using a nonpaired 2-way *t* test.

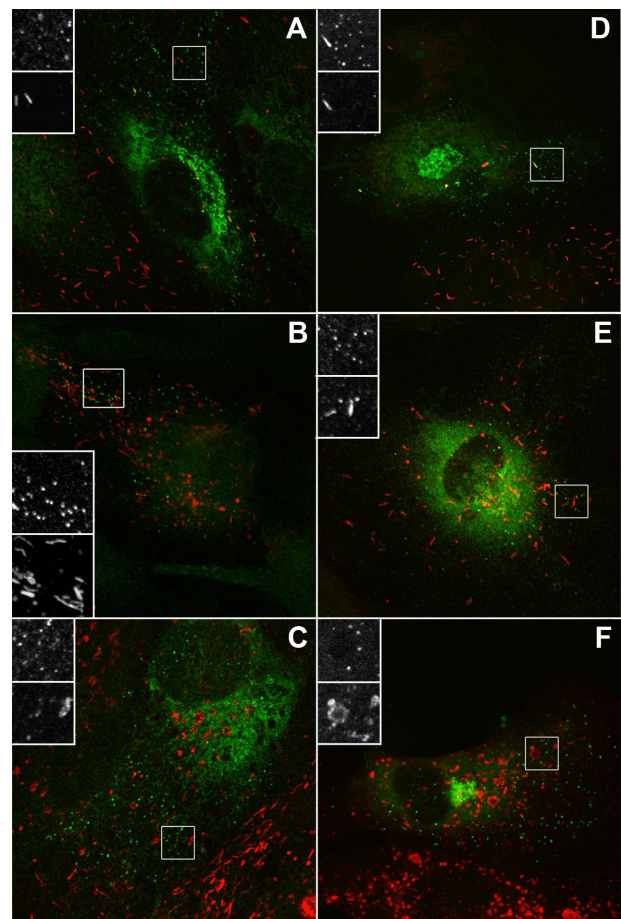


Figure 1. The tPA organelle lacks endogenous VWF, P-selectin, and CD63. (A-C) Representative examples of individual HUVECs labeled with a specific antibody to tPA (green and top panels of grayscale inserts) and VWF (A), P-selectin (B), or CD63 (C) (red and bottom panel of grayscale inserts). (D-F) EGFP fluorescence (green and top panels of grayscale inserts) in cells expressing tPA-EGFP (24 hours after Nucleofection) and counter-labeled with specific antibodies to VWF (D), P-selectin (E), or CD63 (F) (red and bottom panel of grayscale inserts).

Results

Expression of tPA-EGFP labels the endogenous tPA organelle and WPBs in HUVECs

We first compared the subcellular localization of endogenous tPA immunoreactivity or expressed tPA-EGFP fluorescence with WPB marker proteins (VWF, P-selectin, CD63, and Rab27a). Figure 1A-C shows tPA immunoreactivity in HUVECs counterstained for VWF (Figure 1A), P-selectin (Figure 1B), or CD63 (Figure 1C). Figure 1D-F shows tPA-EGFP fluorescence counterstained as in Figure 1A-C. In both cases, numerous small punctate organelles lacking the WPB marker proteins were seen. Endogenous Rab27a was present on WPBs but not punctate tPA-containing organelles (Figure 2A). Coexpression of tPA-EGFP and myc-hRab27a confirmed that punctate tPA-EGFP containing organelles do not recruit Rab27a (Figure 2B). Punctate tPA-EGFP organelles did not colocalize with markers for ER exit sites (myc-sec23), ER to Golgi transport vesicles (Rab1), early and recycling endosomes (transferrin receptor), and lysosomes (Lamp1; data not shown). tPA-EGFP puncta also failed to colocalize with expressed Myc-tagged Rab proteins associated with the Golgi apparatus or constitutive secretory pathway (Rab 6, 8, 10, 11, and 17; data not shown).

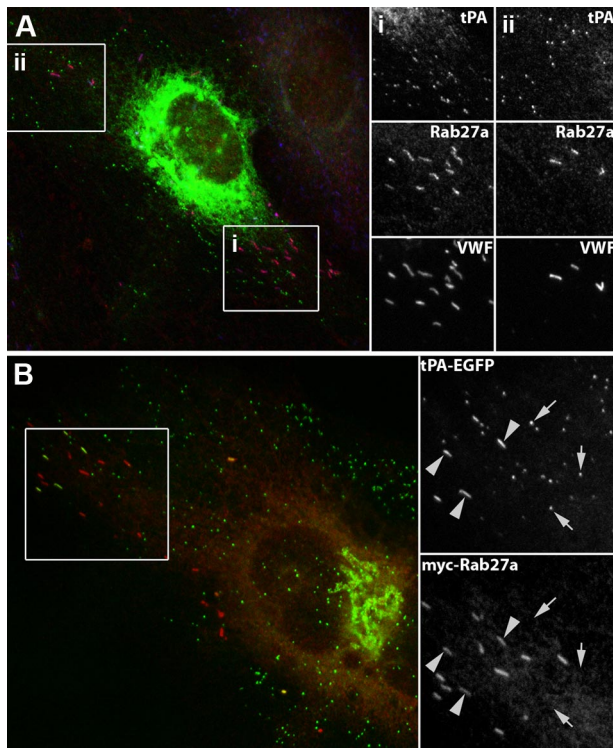


Figure 2. The tPA-EGFP-containing organelle does not recruit endogenous or expressed Rab27a. (A) An individual HUVEC triple labeled with specific antibodies to tPA (green), Rab27a (red), and VWF (blue). Grayscale images of the regions i and ii are shown on the right. (B) Twenty-four hours after Nucleofection with tPA-EGFP (green; EGFP fluorescence) and myc-Rab27a (red). tPA-EGFP is seen in Rab27a-negative puncta and also occasionally in some WPBs, identified by their distinctive rod-shape (large arrowheads). (A-B) Grayscale inserts: regions indicated by white boxes on the color images.

In addition to the small punctate organelles, tPA immunoreactivity (Figure 1A) or expressed tPA-EGFP (Figures 1, 2; supplemental Figure 2) could be observed in some WPBs. The presence of tPA-EGFP in WPBs was dependent on time after Nucleofection; tPA-EGFP was absent from WPBs at early times (4-6 hours; supplemental Figure 2), seen in a variable but small number of WPBs at 24 hours (eg, Figure 1; supplemental Figure 2) and more prominently present in WPBs at 48 hours after Nucleofection (supplemental Figure 2).

The tPA organelle and the type-2 chemokine-containing organelle are the same and can also contain IL-8 or eotaxin-3

A striking and consistent feature in cells expressing tPA-EGFP was the accumulation of fluorescent puncta and material at the Golgi region,^{12,14} illustrated by a close association with the TGN marker protein TGN46 (Figure 3Ai). The same pattern was seen for endogenous tPA immunoreactivity in cells expressing detectable amounts (Figure 3Aii).^{2,3,14} The accumulation of material in or around the Golgi apparatus is also a feature of cytokine up-regulation in ECs^{5,23-25} and was very apparent for GRO- α and MCP-1 in the recent study describing the novel type-2 organelle of ECs.⁵ In that study, transfection with a tPA expression vector failed to produce any visible Golgi accumulation of tPA in the images shown, suggesting that exogenous tPA may not have been expressed correctly in those cells. Down-regulation of endogenous tPA expression in HUVECs by IL-1 β ²⁶ prevented us from directly colocalizing endogenous tPA immunoreactivity within cytokine-containing puncta. Instead, we used exogenous expression of tPA,

tagged with EGFP, allowing independent assessment of expression and localization. tPA-EGFP fluorescence colocalized with punctate GRO- α or MCP-1 immunoreactivity (Figure 2Bi-ii). tPA-EGFP fluorescence also colocalized with punctate endogenous IL-8 or eotaxin-3 immunoreactivity (Figure 2Biii-iv). In IL-4-treated cells, endogenous tPA immunoreactivity colocalized with punctate eotaxin-3 immunoreactivity (supplemental Figure 3A). Exogenously expressed hIL-8 also colocalized with endogenous tPA-containing puncta (supplemental Figure 3B). Triple staining for

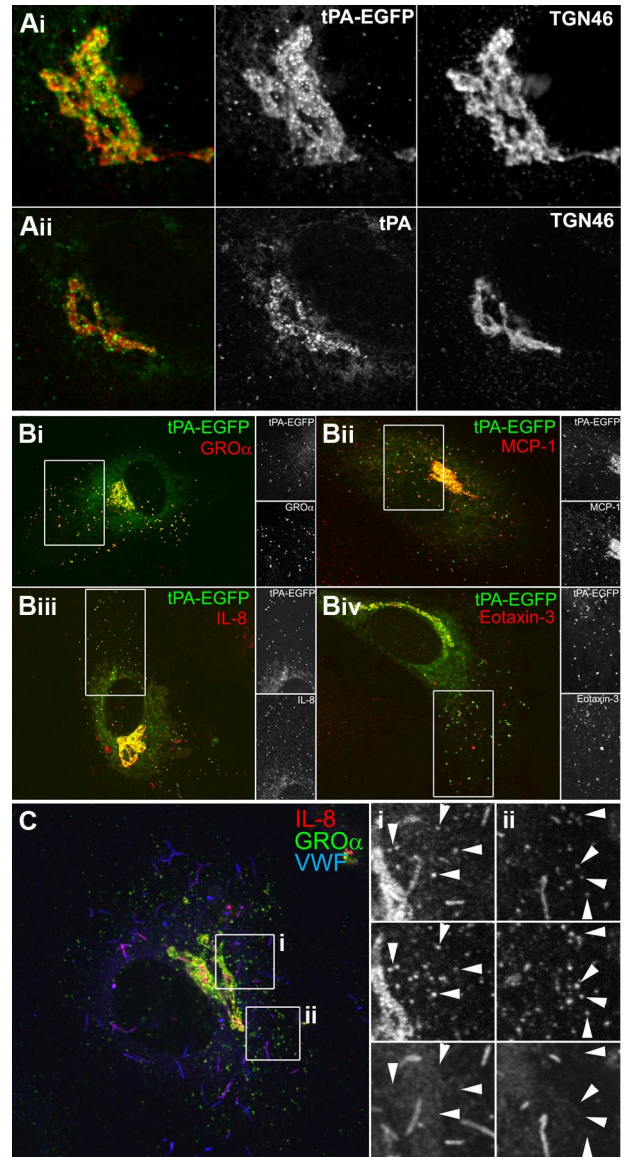


Figure 3. The tPA-EGFP organelle and type-2 organelle are the same. (A) Representative confocal images of the Golgi region of transfected cells expressing tPA-EGFP (Ai; EGFP fluorescence green in color-merged panel) or nontransfected cells labeled for endogenous tPA immunoreactivity (Aii; green in color-merged panel, cells were exposed to 3mM Na butyrate, 24 hours to up-regulate endogenous tPA expression levels¹³) and counterstained with a specific antibody to TGN46 (red in color-merged panels). (B) Cells stained for endogenous GRO- α (i), MCP-1 (ii), IL-8 (iii), or eotaxin-3 (iv) immunoreactivity (red in color-merged images) in cells expressing tPA-EGFP (EGFP fluorescence green in color-merged images). Regions indicated by the white boxes are shown in grayscale to the right of each image. Cells were pretreated with IL-1 β (GRO- α , MCP-1, and IL-8) or IL-4 (eotaxin-3) as described in "Stimulation protocols and ELISAs." (C) IL-8 (red and top panels in grayscale images), GRO- α (green and middle panels in grayscale images), and VWF (blue and bottom panels in grayscale images) immunoreactivity in an IL-1 β -pretreated cell. The white boxes indicate regions shown in grayscale to the right of the color image.

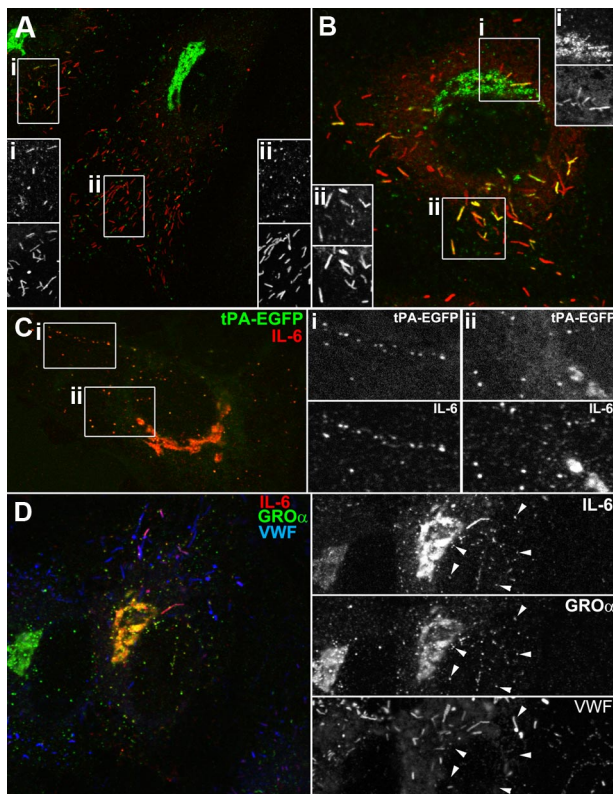


Figure 4. IL-6 is present in the tPA-EGFP organelle and WPBs in IL-1 β -treated cells. (A-B) Examples of single cells labeled for endogenous IL-6 (green in color-merged panels) and endogenous VWF immunoreactivity (red in color-merged panels). (C) Endogenous IL-6 immunoreactivity (red in color-merged image) in a cell expressing tPA-EGFP (EGFP fluorescence green in color-merged image). Regions indicated by the white boxes are shown in grayscale to the right of each image. (D) Endogenous IL-6 (red and top panel in grayscale images), GRO- α (green and middle panel in grayscale images), and VWF (blue and bottom panel in grayscale images) immunoreactivity in an IL-1 β -pretreated cell.

endogenous GRO- α , IL-8, and VWF confirmed that GRO- α and IL-8 are contained within the same small VWF-negative punctate structure (Figure 3Ci-ii small arrows on grayscale insets), although it should be noted that IL-8 was also present in WPBs, consistent with previous reports (Figure 2Ci-ii). We routinely found MCP-1 immunoreactivity in WPBs of IL-1 β -treated cells and low levels of GRO- α in some WPBs (supplemental Figure 3C-D).

IL-6 is present in both the tPA organelle and WPBs in IL-1 β -treated HUVECs

To address whether the tPA organelle might represent a common compartment for inflammatory molecules in ECs exposed to proinflammatory cytokines, we determined the subcellular localization of IL-6, whose endogenous levels are also up-regulated by IL-1²⁷⁻²⁹ (and supplemental Figure 1Aii). After IL-1 β treatment, a large increase in IL-6-specific immunoreactivity was seen in the Golgi region, small puncta, and numerous WPBs (supplemental Figure 4B-C). Figure 4A-B shows in detail the subcellular localization of IL-6 immunoreactivity in individual HUVECs. Expressed tPA-EGFP colocalized with punctate IL-6 immunoreactivity (Figure 4C), and triple staining for GRO- α , IL-6, and VWF confirmed that endogenous GRO- α and IL-6 are contained within the same punctate structures.

The tPA organelle is not a long-term storage organelle

Disruption of ER to Golgi transport by BFA^{30,31} rapidly prevents formation of new secretory granules and was used to probe the

longevity of post-Golgi tPA organelles. Live HUVECs expressing tPA-EGFP 6 hours after Nucleofection were used because at this time point tPA-EGFP was seen only in punctate tPA organelles and not WPBs (supplemental Figure 2). WPBs were studied in separate cells expressing proregion-EGFP. Exposure of HUVECs to 5 μ M BFA led to complete disruption and dispersal of the Golgi apparatus within 5 to 6 minutes (not shown). After 1 hour of BFA treatment, there was no significant effect on numbers of fluorescent WPBs or on basal or histamine-evoked secretion of proregion-EGFP (Figure 5Ai-iv). In contrast, BFA (1 hour) led to a 95% reduction of tPA-EGFP puncta in live cells, with the decrease in puncta after an approximately exponential time course ($\tau = 15.8$ minutes; Figure 5Bi-iii). This was mirrored by a reduction in unstimulated secretion of soluble tPA-EGFP (red symbols in Figure 5Biii-iv) or of soluble GRO- α , MCP-1, and IL-6 determined in separate experiments (Figure 5Biv).

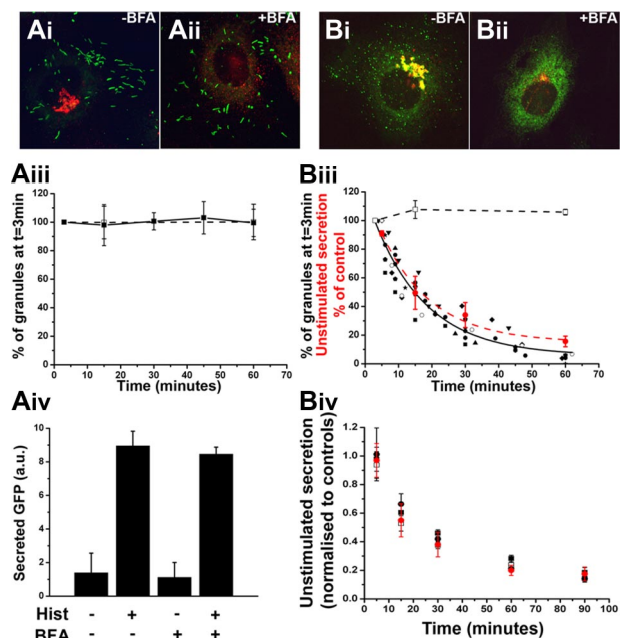


Figure 5. The tPA-EGFP organelle is a short-lived compartment from which unstimulated secretion of tPA-EGFP and cytokines arises. (A-B) Representative examples of fixed cells expressing proregion-EGFP (Ai-ii; 24 hours after Nucleofection) or tPA-EGFP (Bi-ii; 6-7 hours after Nucleofection) and stained with a specific antibody to TGN46 (red in color images) in the absence of BFA (vehicle control; Ai and Bi) or after 1-hour treatment with 5 μ M BFA. Solid squares and line in panel Aiii represent the mean numbers of WPBs, expressed as a percentage of the total number at $t = 3$ minutes after addition of BFA, present in cells at the times indicated ($n = 6$ cells; BFA added at $t = 0$ minutes). Numbers of WPBs in vehicle-treated control cells at 3, 15, and 60 minute time points, expressed in the same way, are shown in open squares with dashed line ($n = 4$ cells). (Biii) Similar data for tPA-EGFP-containing puncta. In this case, the numbers of tPA-EGFP-containing granules in BFA-treated cells are plotted individually because of differences in the precise timing of measurements between experiments ($n = 9$ cells). The solid black line indicates a single exponential decline fitted to the pooled data for all cells. Superimposed on the plot (red circles and red broken line) is the mean decrease in unstimulated secretion of tPA-EGFP in cells treated with BFA. These data are expressed as a percentage of control cells (vehicle-treated) at the times indicated ($n = 4$ independent experiments each carried out in duplicate; BFA added at $t = 0$ minutes). Panels Aiv represent ELISA data for secreted EGFP from cells expressing proregion-EGFP. Cells exposed to BFA or vehicle control (1 hour) were stimulated with histamine or vehicle control (10 minutes) as indicated. Data shown are an individual experiment carried out in triplicate and are representative of 3 separate experiments. Panel Biv represents the mean decrease in unstimulated secretion of IL-6 (\square), GRO- α (\blacksquare), and MCP-1 (\bullet) from IL-1 β -treated cells exposed to BFA at $t = 0$. Data are normalized to that of vehicle control-treated cells at the times indicated and represent data pooled from 3 or 4 independent experiments each carried out in duplicate. For comparison, the data for unstimulated secretion of tPA-EGFP in BFA treated-cells plotted in panel Biii are included in red.

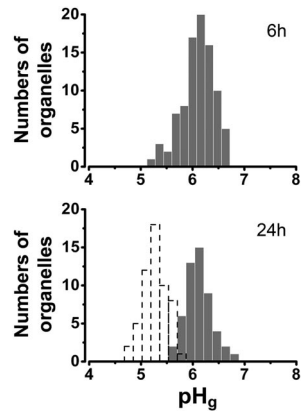


Figure 6. pH in the tPA-EGFP-containing granule. (Top panel) Distribution of pH in tPA-EGFP containing puncta, determined from measurements of individual tPA-EGFP puncta using the NH_4Cl pulse technique¹¹ 6 hours after Nucleofection (mean pH; pH 6.10 ± 0.32 , $n = 89$ organelles, 11 cells). (Bottom panel) Similar data obtained 24 hours after Nucleofection (mean pH; pH 6.11 ± 0.25 , $n = 52$ organelles, 4 cells). The distribution of pH within individual mature WPBs containing tPA-EGFP is shown as a histogram with dashed lines (mean pH; pH 5.27 ± 0.23 , $n = 56$ organelles, 10 cells). Intragranule pH was determined as described in “pH in the tPA organelle.”

The pH within the tPA organelle shows no time-dependent acidification

WPBs are long-lived organelles and undergo substantial intragranule acidification during maturation.¹¹ The short-lived nature of tPA-EGFP puncta led us to suppose that the intragranule pH in these organelles might not be as acidic as that reached by mature WPBs. The intragranule pH for tPA-EGFP-containing organelles was determined using the NH_4Cl pulse technique¹¹ at 6 hours and 24 hours after Nucleofection, and compared with similar values reported for WPBs at these times.¹¹ At 6 hours, tPA-EGFP was exclusively in non-WPB organelles; however, at 24 hours, some WPBs also contained tPA-EGFP (supplemental Figure 2). To distinguish tPA-EGFP-containing WPBs from punctate tPA organelles, cells were cotransfected with proregion-mRFP (that is incorporated into newly formed WPBs) or mRFP-hRab27a (Rab27a is recruited to all mature WPBs³²; and Figure 2). Figure 6 summarizes the distribution of pH in tPA-EGFP puncta at 6 hours and 24 hours, respectively. At both times, the mean pH for individual tPA-EGFP puncta was similar. The mean intra-WPB pH determined using tPA-EGFP 24 hours after Nucleofection (Figure 6 open dashed bars) was similar to that obtained using proregion-EGFP.¹¹

Stimulated secretion and the storage efficiency of tPA and cytokines

Although present in the short-lived punctate organelles, tPA and all cytokines studied here could also be detected within WPBs. We next determined the extent to which these molecules undergo stimulated secretion in the presence or absence of the population of short-lived punctate organelles. Histamine stimulation of Nabutyrate or IL-1 β -treated cells led to a significant increase in the secretion of tPA or IL-8, IL-6, and MCP-1, but not GRO- α (Figure 7Ai-iv). Stimulated secretion of endogenous tPA, IL-8, IL-6, and MCP-1 was maintained after BFA (5 μM , 1-hour) or CHX (5 μM , 24-hour) treatment, conditions where the short-lived punctate organelles were absent (supplemental Figure 5) and unstimulated secretion substantially reduced (Figure 5). Consistent with this, immunofluorescence analysis of BFA- or CHX-treated cells re-

vealed WPBs containing tPA or IL-8, IL-6, MCP-1, or GRO- α (supplemental Figure 5). In CHX-treated cells, ionomycin (1 μM) led to even larger increases in secretion of tPA, IL-8, IL-6, and MCP-1, and reproducibly evoked a small but significant increase in GRO- α secretion (eg, Figure 7Av). Analysis of the storage efficiency of tPA and cytokines revealed that all were very poorly stored within the cells compared with VWF (Figure 7B), irrespective of expression levels (eg, IL-8 storage efficiency was 1%–2% over a 10-fold range of expression produced by IL-1 β , 0.1–10 ng/mL; not shown).

EGFP expressed in the lumen of the secretory pathway appears in WPBs but is poorly stored

The low storage efficiency of cytokines in HUVECs suggested that their presence in WPBs might reflect an inability of the secretory pathway to completely exclude (or subsequently remove) these molecules from nascent WPBs rather than them having “sorting” information specifically directing them into WPBs. If cytokines are found in WPBs simply because they cannot be efficiently excluded, then any nonphysiologic protein should also be stored in WPBs to a similar low degree. Consistent with this, expression of lumEGFP resulted in its incorporation into WPBs (Figure 7C) and was secreted in response to histamine or ionomycin (supplemental Figure 7B). Pulse-chase or ELISA analysis showed that only approximately 4% to 5% of the biosynthetic material was stored (Figure 7B; supplemental Figure 7A).

Discussion

We provide evidence that the tPA organelle and type-2 organelle represent a single compartment responsible for the majority of unstimulated secretion of tPA or cytokines. We suggest that the presence of cytokines and tPA within WPBs arises not from specific sorting to WPBs but rather from an exclusion or removal mechanism that is close to but not 100% efficient. The long-lived nature of WPBs and their accumulation within the cells during periods of high expression of cytokines result in a pool of nonexcluded (missorted) molecules within WPBs that constitute the majority of material available for stimulated secretion.

Unstimulated secretion of tPA-EGFP and cytokines arises from a common compartment

Based on their similar morphology, subcellular distribution, common lack of WPB-specific marker proteins, and depletion after BFA (or CHX) treatment, we conclude that the tPA-EGFP puncta observed here represent the same punctate compartment in which endogenous tPA is found in nontransfected cells. The type-2 chemokine-containing organelle shares a similar morphology, subcellular distribution, and lack of WPB markers; however, its distinct identity was suggested by the failure of overexpressed tPA to colocalize with these organelles.⁵ In that study, there was a conspicuous absence of tPA immunoreactivity in the Golgi region of cells transfected with the tPA-expression vector. Crucially, in our opinion, no epitope tag appears to have been included on the overexpressed tPA that could have independently verified whether the tPA immunoreactivity seen in the transfected cells was the result of transgene expression or endogenous protein. This leads us to propose that, at least in the example shown in Oynebraten et al,⁵ the exogenous tPA may not have expressed (to detectable levels),

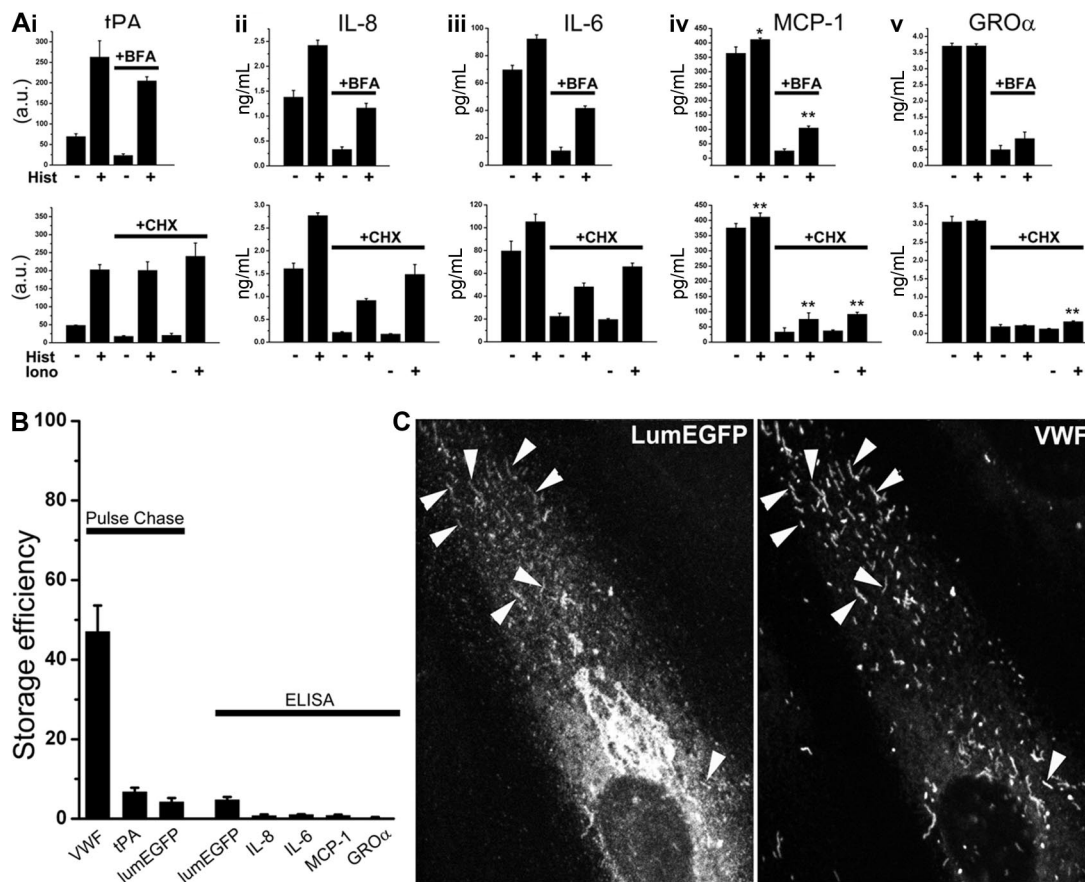


Figure 7. BFA- and CHX-insensitive stimulated secretion and storage efficiency of tPA and cytokines in HUVECs. (A) Top panels: Histamine-stimulated secretion of tPA (i), IL-8 (ii), IL-6 (iii), MCP-1 (iv), and GRO- α (v) in the absence (BFA vehicle, 1 hour) or after BFA treatment (1 hour) as indicated. Cells were pretreated for 24 hours with either 3mM Na-butyrate (i) or 1 ng/mL rhIL-1 β (ii-v) before experiments. Bottom panels: Histamine- or ionomycin-stimulated secretion of tPA and the cytokines in control (CHX vehicle for 24 hours) or CHX-treated (24 hours) cells as indicated. Na-butyrate or rhIL-1 β was included in the media during CHX treatment. Data shown in each case are an individual experiment, carried out in triplicate, and are representative of 3 or 4 replicate experiments. * $P < .05$. ** $P < .001$. (B) Storage efficiency for VWF, tPA, and lumEGFP determined by pulse-chase methodologies and for lumEGFP, IL-8, IL-6, MCP-1, and GRO- α determined by specific ELISA methodologies as indicated. Pulse-chase data in each case are the mean of 2 experiments each carried out in triplicate. Error bars represent the range of the duplicate values. ELISA data are the mean of 3 or 4 separate experiments carried out either in triplicate (LumEGFP) or in duplicate (the cytokines). (C) lumEGFP fluorescence (left panel) and VWF immunoreactivity (right panel) in a cell 48 hours after Nucleofection with lumEGFP. Arrowheads indicate lumEGFP-positive WPBs.

and the peripheral tPA immunoreactivity observed reflected endogenous material synthesized before up-regulation of GRO- α expression by IL-1 β . On the basis of these data, we do not think that an unequivocal discrimination between the type-2 organelle and the tPA organelle is possible.

Here we show, in cells clearly expressing tPA-EGFP, the colocalization of tPA-EGFP with endogenous GRO- α and MCP-1 puncta. tPA-EGFP also colocalized with endogenous IL-8, IL-6, or eotaxin-3 puncta. Exogenously expressed IL-8 colocalized with endogenous tPA puncta, as did endogenous eotaxin-3. Colocalization of endogenous GRO- α -containing, VWF-negative puncta with endogenous IL-8 or IL-6 puncta suggests that this small punctate organelle represents a common compartment for many small molecules whose expression is up-regulated by inflammatory cytokines. The appearance of cytokine-containing puncta in IL-1 β -treated cells is accompanied by a large increase in unstimulated secretion of these molecules (Figure 7; supplemental Figure 1). Unstimulated exocytosis of punctate tPA-EGFP organelles in ECs (14 and supplemental Figure 6) suggests that these organelles could represent a pathway primarily responsible for unstimulated secretion. Data presented in Figure 4 show that this is the case. The exponential time course for loss of these granules after BFA treatment indicates that the final plasma membrane fusion step in unstimulated exocytosis is not rate limiting; this organelle is not a

true storage organelle like the WPB. Consistent with its short life-time, the intra-tPA organelle pH was similar to that of the TGN (\sim pH 6.2)³³ and showed no evidence of further acidification as seen for WPBs.¹¹

The majority of stimulated cytokine secretion arises from WPBs

We found MCP-1 in WPBs, and also GRO- α , although its levels were very low and often difficult to detect because of the numerous small punctate organelles (supplemental Figures 3B, 5). Their presence in WPBs was most clearly revealed after depletion of punctate organelles by BFA or CHX treatment (supplemental Figure 5). IL-6 was also present in WPBs in a pattern similar to that reported for IL-8 and eotaxin-3.^{24,25} Consistent with this, histamine- or ionomycin-evoked secretion of IL-8, IL-6, MCP-1, and tPA persisted largely unaltered after BFA or CHX treatment. n-Butanol, a partial but selective inhibitor of WPB exocytosis,¹² partially inhibited stimulated secretion of tPA, IL-8, and the VWF-propolypeptide in BFA-treated cells (supplemental Figure 8), consistent with this secreted material arising from WPBs. A weak stimulated secretion of GRO- α was only seen in response to ionomycin in CHX-treated cells, consistent with very low levels of GRO- α immunoreactivity seen in some WPBs. These data imply that exocytosis of the small punctate organelles is either insensitive

or only very weakly sensitive to secretagogue stimulation. To examine this, we imaged live cells expressing tPA-EGFP (and proregion-mRFP or mRFP-Rab27a to mark tPA-EGFP containing WPBs) or proregion-EGFP alone (a specific WPB marker). In approximately 50% of the cells studied, stimulation with histamine or ionomycin failed to evoke fusion of tPA-EGFP puncta. In the remaining cells, a variable but weak response was seen comprising fusion of approximately 1% to 5% of the fluorescent puncta (supplemental Figure 6). The perfusion pH values within these organelles (supplemental Figure 6C), determined by epifluorescence measurements,¹¹ were similar to those determined using NH₄Cl (Figure 6). In contrast, WPB exocytosis was seen in all cells studied with approximately 70% degranulation during strong stimulation (supplemental Figure 6). Together, the ELISA and live cell imaging data confirm that the majority of stimulated secretion of cytokines and tPA arises from WPB exocytosis. The small punctate organelle is at best poorly responsive to histamine or ionomycin.

Are cytokines sorted to or excluded from the WPBs? Identification of IL-8 and eotaxin-3 in WPBs has led to the suggestion that these soluble molecules are “sorted” into this organelle,^{5,23,24,34} perhaps through interactions with VWF.²³ Other soluble molecules that bind VWF and are detectable in WPBs include osteoprotegerin and factor VIII,³⁵⁻³⁷ raising the attractive idea that VWF may act as a molecular chaperone for sorting to WPBs. However, an elegant series of studies have shown that binding of factor VIII to VWF plays no role in its inclusion in WPBs.^{38,39} Thus, VWF binding does not necessarily play a role in the entry of molecules to WPBs. Evidence presented here and from other studies suggests that the cytokines or tPA may not be actively sorted to WPBs but instead are not completely excluded from these organelles. First, the majority of cytokine material produced after up-regulation by IL-1 β is not stored within the cells (Figure 7). Consistent with this, pulse-chase experiments show that virtually all de novo produced IL-8 is secreted from ECs within approximately 60 minutes of its synthesis.²³ Similar results have been reported for tPA⁴⁰ and were confirmed here (Figure 7). Because cytokine immunoreactivity could also be seen in non-WPB compartments (eg, Golgi associated) after CHX treatment (supplemental Figure 5), the amount of material specifically in WPBs probably represents only a fraction of the approximate 1% of cell-associated (stored) material (Figure 7B). In comparison, the storage efficiency of VWF was approximately 50% (Figure 7B). Thus, if cytokines or tPA are sorted to WPBs, this process is very inefficient, and is no more efficient than that of a nonmammalian nonsecretory protein (lumEGFP) targeted to the secretory pathway (Figure 7B-C).

Two models for sorting of soluble luminal proteins to regulated secretory granules have been postulated.^{41,42} The “sorting for entry” model postulates specific mechanisms directing soluble proteins into immature secretory granules during their formation,

whereas the “sorting by retention” model postulates that entry of proteins into immature secretory granules is not particularly selective. In the latter model, the final composition of the organelle depends on processes, such as cargo aggregation and the removal of soluble proteins from the organelle during its maturation. It is now clear that many, if not all, proteins destined largely for constitutive secretion can enter newly forming regulated secretory granules without the need for specific sorting signals.^{41,43} In pancreatic β -cells, no endogenous secretory protein specific only to the constitutive pathway has yet been identified.⁴³ The data presented here are consistent with such a model and are supported by our observation that lumEGFP can enter WPBs, and similar data showing that nonsecretory proteins, when directed into the ER, can enter the regulated secretory pathway.⁴¹ The very low level of retention of molecules, such as IL-8, may arise through weak binding to VWF,²³ nonspecific entrapment within the condensing proregion-VWF paracrystal,⁴⁴ or incomplete removal during organelle maturation. Fluorescence recovery after photobleaching analysis of eotaxin-3-EGFP and lumEGFP has shown that these molecules diffuse freely in the immature WPBs, suggesting they enter via and remain in the fluid phase.⁴⁵

According to the simple model outlined in the preceding paragraph, molecules such as IL-8, IL-6, GRO- α , MCP-1, and eotaxin-3 and tPA are destined primarily for unstimulated secretion but enter the WPBs because of an exclusion or removal mechanism that is not quite (but almost) 100% efficient. If this is the case, then the presence of such molecules in WPBs reflects missorting and has implications for how we view the physiologic or pathophysiologic roles of such molecules when secreted from WPBs.

Acknowledgments

T.C. and M.J.H. were supported by the Medical Research Council (reference codes U117573808 and U117570589).

Authorship

Contribution: L.K., A.M., L.H., M.J.H., R.B., and T.C. performed research and analyzed data; P.S., M.J.H., and J.D. contributed reagents/analytical tools; and T.C. designed the research and wrote the paper.

Conflict-of-interest disclosure: The authors declare no competing financial interests.

The current affiliation for A.M. is Faculty of Medicine, Imperial College, London, United Kingdom.

Correspondence: Tom Carter, National Institute for Medical Research, Mill Hill, London NW7 1AA, United Kingdom; e-mail: tcarter@nimr.mrc.ac.uk.

References

- Sadler JE. Biochemistry and genetics of von Willebrand factor. *Annu Rev Biochem*. 1998;67:395-424.
- Emeis JJ, van den Eijnden-Schrauwen Y, van den Hoogen CM, de Priester W, Westmuckett A, Lupu F. An endothelial storage granule for tissue-type plasminogen activator. *J Cell Biol*. 1997;139(1):245-256.
- Knop M, Aareskjold E, Bode G, Gerke V. Rab3D and annexin A2 play a role in regulated secretion of vWF, but not tPA, from endothelial cells. *EMBO J*. 2004;23(15):2982-2992.
- Kooistra T, Schrauwen Y, Arts J, Emeis JJ. Regulation of endothelial cell t-PA synthesis and release. *Int J Hematol*. 1994;59(4):233-255.
- Oynebraten I, Barois N, Hagelsteen K, Johansen FE, Bakke O, Haraldsen G. Characterization of a novel chemokine-containing storage granule in endothelial cells: evidence for preferential exocytosis mediated by protein kinase A and diacylglycerol. *J Immunol*. 2005;175(8):5358-5369.
- Bauerfeind R, Jelinek R, Hellwig A, Huttner WB. Neurosecretory vesicles can be hybrids of synaptic vesicles and secretory granules. *Proc Natl Acad Sci U S A*. 1995;92(16):7342-7346.
- Borregaard N, Cowland JB. Granules of the human neutrophilic polymorphonuclear leukocyte. *Blood*. 1997;89(10):3503-3521.
- Italiano JE Jr, Richardson JL, Patel-Hett S, et al. Angiogenesis is regulated by a novel mechanism: pro- and antiangiogenic proteins are organized into separate platelet alpha granules and differentially released. *Blood*. 2008;111(3):1227-1233.
- Wagner DD. Cell biology of von Willebrand factor. *Annu Rev Cell Biol*. 1990;6:217-246.

10. Gibling JP, Hewlett LJ, Hannah MJ. Basal secretion of von Willebrand factor from human endothelial cells. *Blood*. 2008;112(4):957-964.
11. Erent M, Meli A, Moiso N, et al. Rate, extent and concentration-dependence of histamine-evoked Weibel-Palade body exocytosis determined from individual fusion events in human endothelial cells. *J Physiol*. 2007;583:195-212.
12. Disse J, Vitale N, Bader MF, Gerke V. Phospholipase D1 is specifically required for regulated secretion of von Willebrand factor from endothelial cells. *Blood*. 2009;113(4):973-980.
13. Huber D, Cramer EM, Kaufmann JE, et al. Tissue-type plasminogen activator (t-PA) is stored in Weibel-Palade bodies in human endothelial cells both in vitro and in vivo. *Blood*. 2002;99(10):3637-3645.
14. Suzuki Y, Mogami H, Ihara H, Urano T. Unique secretory dynamics of tissue plasminogen activator and its modulation by plasminogen activator inhibitor-1 in vascular endothelial cells. *Blood*. 2009;113(2):470-478.
15. Babich V, Meli A, Knipe L, et al. Selective release of molecules from Weibel Palade bodies during a lingering kiss. *Blood*. 2008;111(11):5282-5290.
16. Hannah MJ, Skehel P, Erent M, Knipe L, Ogden D, Carter T. Differential kinetics of cell surface loss of von Willebrand factor and its propolypeptide after secretion from Weibel-Palade bodies in living human endothelial cells. *J Biol Chem*. 2005;280(24):22827-22830.
17. Manneville JB, Etienne-Manneville S, Skehel P, Carter T, Ogden D, Ferenczi M. Interaction of the actin cytoskeleton with microtubules regulates secretory organelle movement near the plasma membrane in human endothelial cells. *J Cell Sci*. 2003;116(19):3927-3938.
18. Babich V, Knipe L, Hewlett L, et al. Differential effect of extracellular acidosis on the release and dispersal of soluble and membrane proteins secreted from the Weibel-Palade body. *J Biol Chem*. 2009;284(18):12459-12468.
19. Blum R, Stephens DJ, Schulz I. Luminal targeted GFP, used as a marker of soluble cargo, visualises rapid ERGIC to Golgi traffic by a tubulovesicular network. *J Cell Sci*. 2000;113(18):3151-3159.
20. Moore HP, Kelly RB. Secretory protein targeting in a pituitary cell line: differential transport of foreign secretory proteins to distinct secretory pathways. *J Cell Biol*. 1985;101(5):1773-1781.
21. Mashanov GI, Knipe L, Molloy JE, Carter T. Single fluorophore tracking of P-selectin-EGFP during exocytosis of Weibel-Palade bodies. *Eur Biophys J*. 2007;36[suppl 1]:S178.
22. Mashanov GI, Tacon D, Knight AE, Peckham M, Molloy JE. Visualizing single molecules inside living cells using total internal reflection fluorescence microscopy. *Methods*. 2003;29(2):142-152.
23. Bierings R, van den Biggelaar M, Kragt A, Mertens K, Voorberg J, van Mourik JA. Efficiency of von Willebrand factor-mediated targeting of interleukin-8 into Weibel-Palade bodies. *J Thromb Haemost*. 2007;5(12):2512-2519.
24. Oynebraten I, Bakke O, Brandtzaeg P, Johansen FE, Haraldsen G. Rapid chemokine secretion from endothelial cells originates from 2 distinct compartments. *Blood*. 2004;104(2):314-320.
25. Wolff B, Burns AR, Middleton J, Rot A. Endothelial cell "memory" of inflammatory stimulation: human venular endothelial cells store interleukin 8 in Weibel-Palade bodies. *J Exp Med*. 1998;188(9):1757-1762.
26. Larsson P, Ulfhammer E, Karlsson L, Bokarewa M, Wahlander K, Jern S. Effects of IL-1beta and IL-6 on tissue-type plasminogen activator expression in vascular endothelial cells. *Thromb Res*. 2008;123(2):342-351.
27. Kaplanski G, Teyssie N, Farnarier C, et al. IL-6 and IL-8 production from cultured human endothelial cells stimulated by infection with Rickettsia conorii via a cell-associated IL-1 alpha-dependent pathway. *J Clin Invest*. 1995;96(6):2839-2844.
28. Nilsen EM, Johansen FE, Jahnsen FL, et al. Cytokine profiles of cultured microvascular endothelial cells from the human intestine. *Gut*. 1998;42(5):635-642.
29. Sironi M, Breviaro F, Proserpio P, et al. IL-1 stimulates IL-6 production in endothelial cells. *J Immunol*. 1989;142(2):549-553.
30. Lippincott-Schwartz J, Yuan LC, Bonifacino JS, Klausner RD. Rapid redistribution of Golgi proteins into the ER in cells treated with brefeldin A: evidence for membrane cycling from Golgi to ER. *Cell*. 1989;56(5):801-813.
31. Mantei N, Villa M, Enzler T, et al. Complete primary structure of human and rabbit lactase-phlorizin hydrolase: implications for biosynthesis, membrane anchoring and evolution of the enzyme. *EMBO J*. 1988;7(9):2705-2713.
32. Hannah MJ, Hume AN, Arribas M, et al. Weibel-Palade bodies recruit Rab27 by a content-driven, maturation-dependent mechanism that is independent of cell type. *J Cell Sci*. 2003;116(19):3939-3948.
33. Paroutis P, Touret N, Grinstein S. The pH of the secretory pathway: measurement, determinants, and regulation. *Physiology (Bethesda)*. 2004;19:207-215.
34. Hol J, Kuchler AM, Johansen FE, Dalhus B, Haraldsen G, Oynebraten I. Molecular requirements for sorting of the chemokine interleukin-8/CXCL8 to endothelial Weibel-Palade bodies. *J Biol Chem*. 2009;284(35):23532-23539.
35. Shahbazi S, Lenting PJ, Fribourg C, Terraube V, Denis CV, Christophe OD. Characterization of the interaction between von Willebrand factor and osteoprotegerin. *J Thromb Haemost*. 2007;5(9):1956-1962.
36. Zannettino AC, Holding CA, Diamond P, et al. Osteoprotegerin (OPG) is localized to the Weibel-Palade bodies of human vascular endothelial cells and is physically associated with von Willebrand factor. *J Cell Physiol*. 2005;204(2):714-723.
37. Rosenberg JB, Foster PA, Kaufman RJ, et al. Intracellular trafficking of factor VIII to von Willebrand factor storage granules. *J Clin Invest*. 1998;101(3):613-624.
38. van den Biggelaar M, Meijer AB, Voorberg J, Mertens K. Intracellular cotrafficking of factor VIII and von Willebrand factor type 2N variants to storage organelles. *Blood*. 2009;113(13):3102-3109.
39. van den Biggelaar M, Bierings R, Storm G, Voorberg J, Mertens K. Requirements for cellular co-trafficking of factor VIII and von Willebrand factor to Weibel-Palade bodies. *J Thromb Haemost*. 2007;5(11):2235-2242.
40. van den Eijnden-Schrauwen Y, Kooistra T, de Vries RE, Emeis JJ. Studies on the acute release of tissue-type plasminogen activator from human endothelial cells in vitro and in rats in vivo: evidence for a dynamic storage pool. *Blood*. 1995;85(12):3510-3517.
41. Arvan P, Castle D. Sorting and storage during secretory granule biogenesis: looking backward and looking forward. *Biochem J*. 1998;332(3):593-610.
42. Arvan P, Halban PA. Sorting ourselves out: seeking consensus on trafficking in the beta-cell. *Traffic*. 2004;5(1):53-61.
43. Lara-Lemus R, Liu M, Turner MD, et al. Luminal protein sorting to the constitutive secretory pathway of a regulated secretory cell. *J Cell Sci*. 2006;119(9):1833-1842.
44. Berriman JA, Li S, Hewlett LJ, et al. Structural organization of Weibel-Palade bodies revealed by cryo-EM of vitrified endothelial cells. *Proc Natl Acad Sci U S A*. 2009;106(41):17407-17412.
45. Kiskin NI, Hellen N, Babich V, et al. Protein mobilities and P-selectin storage in Weibel-Palade bodies. *J Cell Sci*. 2010;123(Pt 17):2964-2975.